# Holographic QCD methods for meson production

**Kiminad Mamo** (William & Mary)

July 28, 2025 @ Towards improved hadron femtography with hard exclusive reactions, edition IV, Jefferson Lab

# References

This talk is based on:

- **1910.04707** (PRD) (with Ismail Zahed)
- **2106.00722** (PRD) (with Ismail Zahed)
- **2204.08857** (PRD) (with Ismail Zahed)
- **2206.03813** (PRD) (with Ismail Zahed)
- **25xx.xxxxx** (In Preparation) (with Christian Weiss)

# AdS/CFT

- The AdS/CFT correspondence can be used to compute correlation functions of local operators [Maldacena (1998); Gubser, Klebanov, Polyakov (1998); Witten (1998)]:

$$Z_{\rm gauge}(J\mathcal{O}, N_c, \lambda) \;\equiv\; Z_{\rm gravity}(\phi_0, g_5, \alpha'/R^2), \quad \text{where } J \equiv \phi_0.$$

- Correlation functions are evaluated via Witten diagrams in $\mathrm{AdS}$.
- For non-conformal theories with a mass gap (dual to a deformed AdS background), scattering amplitudes can likewise be computed using these Witten diagrams in AdS

$$ds^2 = \frac{R^2}{z^2}\left(\eta_{\mu\nu}\, dx^\mu dx^\nu - dz^2\right), \quad \eta_{\mu\nu} = \mathrm{diag}(1,-1,-1,-1),$$

with $0 \leq z \leq \infty$, connects the UV boundary ($z \to 0$) to the IR ($z \to \infty$), and mass gap/confinement induced by a background dilaton field $\phi(z) = \kappa^2 z^2$.

# Two-point function

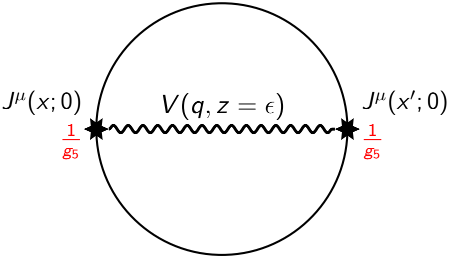


Figure: Witten diagram for the two-point function of the current operator with $g_5^2 \sim \frac{1}{N_c}$.

- The bulk-to-boundary propagator for the virtual photon is

$$\mathcal{V}(Q,z) = g_5 \sum_n \frac{F_n\,\phi_n(z)}{Q^2+m_n^2} = \Gamma\left(1+\frac{Q^2}{4\kappa^2}\right)\kappa^2 z^2\,\mathcal{U}\left(1+\frac{Q^2}{4\kappa^2};2;\kappa^2 z^2\right),$$

where $\Gamma$ is the Gamma function and $\mathcal{U}$ is the Tricomi confluent hypergeometric function.

# Spin-1 (Electromagnetic) Form Factors of Proton

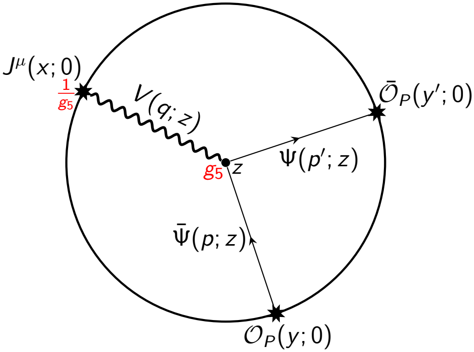


Figure: Witten diagram for EM form factor due to the exchange of vector mesons with $g_5^2 \sim \frac{1}{N_c}$.

# Spin-1 (Electromagnetic) Form Factors of Proton

- The scattering amplitude in AdS is

$$S^{EM}_{Dirac}[i,f] \;=\; (2\pi)^4\,\delta^4(p'-p-q)\,\frac{1}{g_5}\;\times g_5\,\overline{u}_{s_f}(p')\,\epsilon_\mu(q)\gamma^\mu\,u_{s_i}(p)$$

$$\times\frac{1}{2}\int\frac{dz}{z^{2M}}\,e^{-\phi}\,\mathcal{V}(Q,z)\left(\psi_L^2(z)+\psi_R^2(z)\right).$$

# Spin-2/0 (Gravitational) Form Factors of Proton

- The gravitational form factors (GFFs) of the proton are defined via the energy-momentum tensor (EMT):

$$\langle p_2 \mid T^{\mu\nu}(0) \mid p_1 \rangle = \overline{u}(p_2)\left( A(k)\gamma^{(\mu} p^{\nu)} + B(k)\,\frac{i\,p^{(\mu}\sigma^{\nu)\alpha} k_\alpha}{2m_N} + C(k)\,\frac{k^\mu k^\nu - \eta^{\mu\nu} k^2}{m_N} \right) u(p_1),$$

with $k = p_2 - p_1$. Often one writes $D(k) \equiv 4\,C(k)$.

- The bulk metric fluctuations decompose into spin-2 (transvers-traceless part $h$) and spin-0 (traceful part $f$) [Kanitscheider (2008)]:

$$h_{\mu\nu}(k,z) \supset \left[\epsilon^{TT}_{\mu\nu}\, h(k,z)\right] + \left[\tfrac{1}{3}\,\eta_{\mu\nu}\, f(k,z)\right].$$

- For non-degenerate $2^{++}$ and $0^{++}$ glueball spectra, the holographic coupling includes both transverse-traceless (spin-2) and scalar (spin-0) fluctuations, respectively.

# Spin-2/0 (Gravitational) Form Factors of Proton

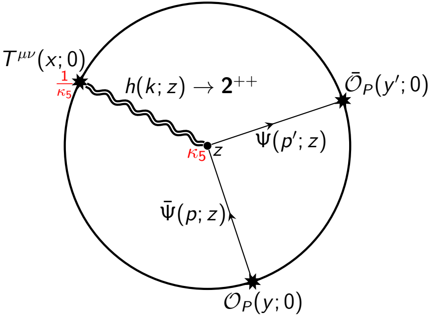


Figure: Witten diagram for spin-2 gravitational form factor due to the exchange $2^{++}$ glueballs with $\kappa_5^2 \sim \frac{1}{N_c^2}$.

$$A(K,\kappa_T) \;=\; \frac{1}{2}\int dz\,\sqrt{g}\,e^{-\phi}\,z\left(\psi_R^2(z)+\psi_L^2(z)\right)\sum_{n=0}^{\infty}\frac{\sqrt{2}\,\kappa_5\,F_n\,\psi_n(z)}{K^2+m_n^2}.$$

# Holographic Gravitational Form Factors

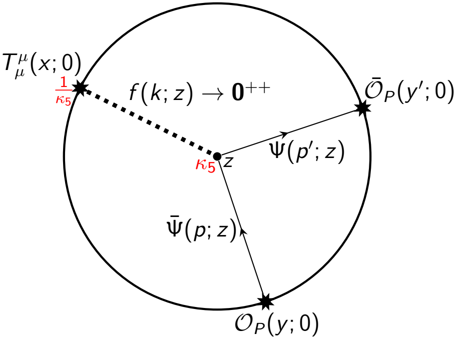


Figure: Witten diagram for scalar gravitational form factor due to the exchange $0^{++}$ glueballs.

$$D(K,\kappa_T,\kappa_S) = -\frac{4\,m_N^2}{3\,K^2}\Big[A(K,\kappa_T)\;-\;A_S(K,\kappa_S)\Big],$$

# Comparison with Lattice Data

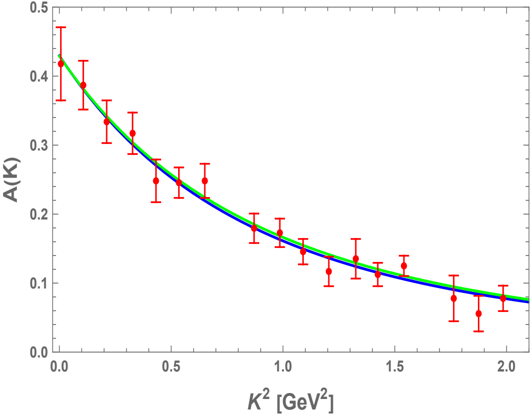


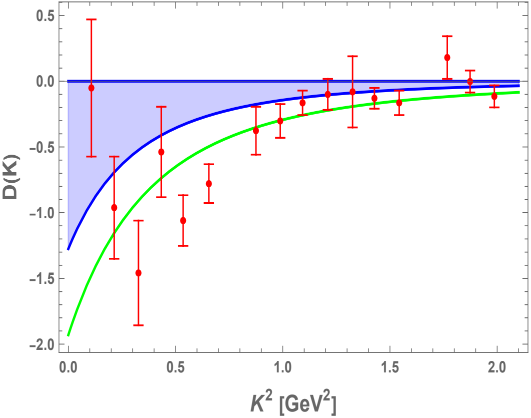

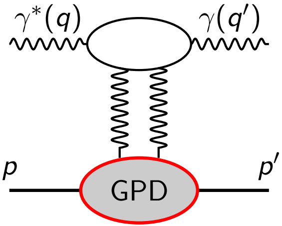


collinear factorization

$\equiv$

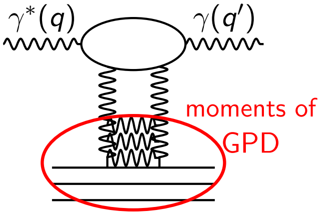


with BFKL kernel

$\equiv$

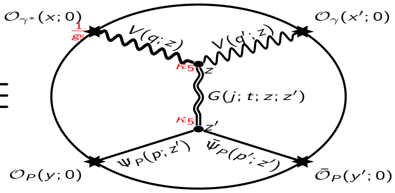


with BPST (holographic) kernel

- the scattering amplitude using the BFKL kernel:

$$\mathrm{Im}\,\mathcal{A}_{\gamma^*_{L/T} p \to Vp}(j,s,t) = \int_0^\infty k_\perp\, k_\perp \int_{k_\perp}^\infty k'_\perp\, k'\ \Phi_A(k_\perp, Q)\, G(j;t;k_\perp;k'_\perp)\, \Phi_B(k'_\perp)\,,$$

$$\mathrm{Im}\,\mathcal{A}_{\gamma^*_{L/T} p \to Vp}(s,t) = \int_{C-i\infty}^{C+i\infty} \frac{j}{2\pi i} \left(\frac{s}{s_0}\right)^{j-1} I(j,Q) \times F(j,t)$$

# Four-point correlation functions $< \bar{P} J_\mu J_\nu P >$ with spin-j exchange

| **Feature** | **BFKL** ($\lambda \ll 1$) | **BPST** ($\lambda \gg 1$) |
|---|---|---|
| Transverse variable | $k_\perp$ | $z \propto k_\perp$ |
| Differential kernel | $k_\perp^2 \partial_{k_\perp}^2 + k_\perp \partial_{k_\perp} - \frac{4}{D_p}(j - j_0^p)$ | $k_\perp^2 \partial_{k_\perp}^2 + k_\perp \partial_{k_\perp} - \frac{4}{D_h}(j - j_0^h)$ |
| Intercept shift | $j_0^p = 1 + \frac{\lambda \ln 2}{\pi^2}$ | $j_0^h = 2 - \frac{2}{\sqrt{\lambda}}$ |
| Diffusion width | $D_p = \frac{7\,\zeta(3)}{2\pi^2}\lambda$ | $D_h = \frac{2}{\sqrt{\lambda}}$ |

# Four-point correlation functions $< \bar{P} J_\mu J_\nu P >$ with spin-j exchange

- the scattering amplitude using the holographic kernel:

$$\mathcal{A}_{\gamma^*_{L/T} p \to Vp}(j,s,t,Q^2) \sim -\frac{1}{g_5} \times 2\kappa^2 \times \mathcal{V}_{h\gamma^*_{L/T} V}(j,Q) \times \mathcal{V}_{h\bar{\Psi}\Psi}(j,t) \\ \times \left[ q^{\mu_1} q^{\mu_2} \ldots q^{\mu_j} \, P_{\mu_1\mu_2\ldots\mu_j;\nu_1\nu_2\ldots\nu_j}(k) \, p_1^{\nu_1} p_1^{\nu_2} \ldots p_1^{\nu_j} \right] \\ \times \frac{1}{m_N} \times \bar{u}(p_2) u(p_1)$$

- the summation over all spin-$j$ glueball/meson exchanges is performed using the Sommerfeld–Watson formula

$$\mathcal{A}^{tot}_{\gamma^* p \to V/\pi^0 p}(s,t,Q^2) = -\int_{\mathbb{C}} \frac{dj}{2\pi i} \frac{s^j \pm (-s)^j}{\sin(\pi j)} \mathcal{A}_{\gamma^* p \to \pi^0/Vp}(j,s,t,Q^2),$$

where the contour $\mathbb{C}$ is taken to the left of all even or odd poles (See **Kemal**'s talk on Wednesday)

# Photoproduction of Heavy Mesons Near Threshold

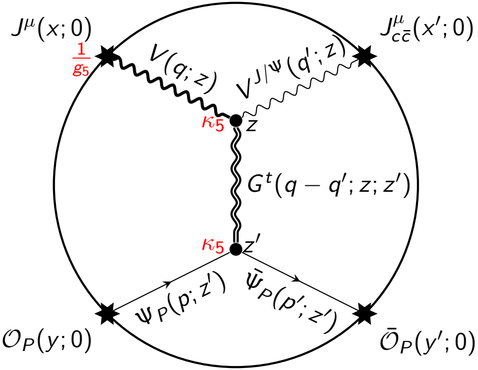


Figure: Witten diagrams for the holographic photo/electroproduction of $J/\Psi$ with $g_5^2 \sim \frac{1}{N_c}$ and $\kappa_5^2 \sim \frac{1}{N_c^2}$.

# Photoproduction of heavy mesons near threshold

- the differential cross section for photoproduction of heavy vector mesons ($J/\psi$ or $\Upsilon$), near threshold, is given by

$$\begin{aligned}\frac{d\sigma}{dt} &= \mathcal{N}^2 \times \left[A(t) + \eta^2 D(t)\right]^2 \\ &\times \frac{1}{A^2(0)} \times \frac{1}{32\pi(s-m_N^2)^2} \times F(s,t,M_V,m_N) \times \left(1 - \frac{t}{4m_N^2}\right)\end{aligned}$$

with the normalization factor $\mathcal{N}$ defined as

$$\mathcal{N}^2 \equiv e^2 \times \left(\frac{f_V}{M_V}\right)^2 \times \mathbb{V}^2_{h\gamma^* J/\Psi} \times (2\kappa_5^2)^2 \times A^2(0) = 7.768^2\,\mathrm{nb}/\mathrm{GeV}^6$$

- note that $F(s,t) \sim s^4 \sim 1/\eta^4$ with the amplitude $\mathcal{A} \sim s^2 \times A(t) + s^0 \times D(t)$ as expected from $2^{++}$ and $0^{++}$ glueball t-channel exchanges

# Extraction of the $2^{++}$ glueball contribution

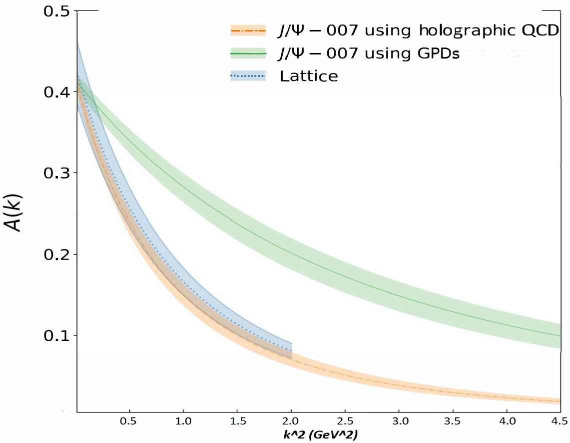


Figure: The extracted $A(-t)$ form factor from $\gamma p \to J/\psi\, p$ near threshold, as measured by the J/$\psi$-007 Collaboration at JLab [Duran et al. (Nature, 2022)].

# Extraction of the $0^{++}$ glueball contribution

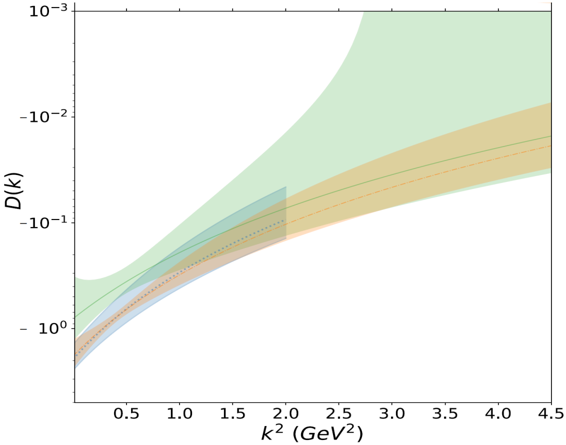


Figure: Similarly, the extracted $D(-t)$ (or $4C(-t)$) form factor from near-threshold photoproduction at JLab.

# Electroproduction of heavy mesons near threshold

- the differential cross section for electroproduction of heavy vector mesons ($J/\psi$ or $\Upsilon$), near threshold, is given by

$$\begin{aligned}
\frac{d\sigma(s,t,Q,M_{J/\Psi},\epsilon_T,\epsilon'_T)}{dt} &\propto \mathcal{I}^2(Q,M_{J/\Psi}) \times \left(\frac{s}{\kappa^2}\right)^2 \times \left[A(t)+\eta^2 D(t)\right]^2 \\
\frac{d\sigma(s,t,Q,M_{J/\Psi},\epsilon_L,\epsilon'_L)}{dt} &\propto \frac{1}{9} \times \frac{Q^2}{M^2_{J/\Psi}} \times \mathcal{I}^2(Q,M_{J/\Psi}) \times \left(\frac{s}{\kappa^2}\right)^2 \times \left[A(t)+\eta^2 D(t)\right]^2
\end{aligned}$$

# Electroproduction of heavy mesons near threshold

- where we defined the transition form factor that controls the $Q$ dependence as

$$\mathcal{I}(Q, M_{J/\Psi}) = \frac{\mathcal{I}(0, M_{J/\Psi})}{\frac{1}{6} \times \left(\frac{Q^2}{4\kappa_{J/\Psi}^2} + 3\right)\left(\frac{Q^2}{4\kappa_{J/\Psi}^2} + 2\right)\left(\frac{Q^2}{4\kappa_{J/\Psi}^2} + 1\right)},$$

with $\mathcal{I}(0, M_{J/\Psi}) = \frac{g_5 f_{J/\Psi}}{4M_{J/\Psi}}$

# Electroproduction of heavy mesons near threshold

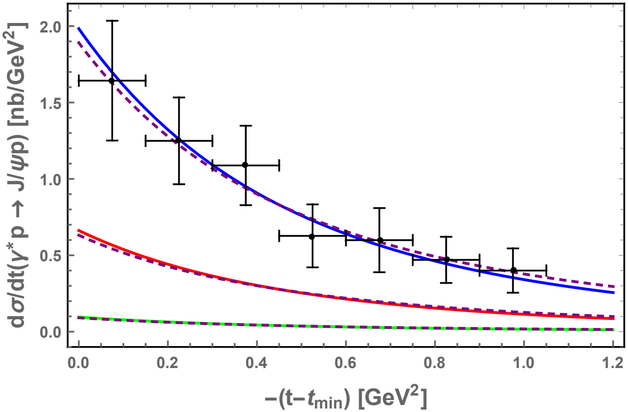


Figure: The variation of the total differential cross section with $t$ and $Q^2$ for $s = 21\ GeV^2$. The blue curve is for $Q = 0$. The red curve is for $Q = 1.2\ GeV$. The green curve is for $Q = 2.2\ GeV$. The data is from GlueX collaboration at JLab in 2019.

# Electroproduction of heavy mesons near threshold

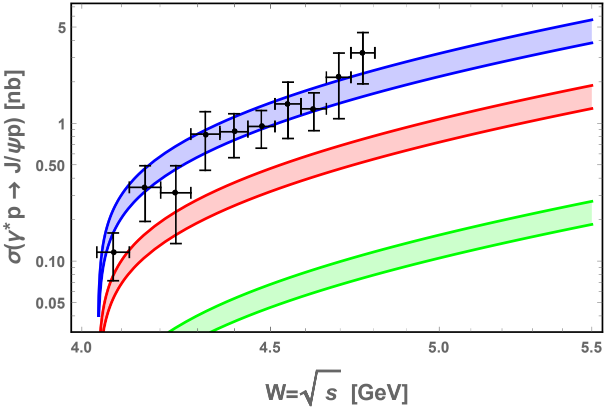


Figure: The variation of the total cross section (near threshold) with $Q^2$ and $\sqrt{s}$. The blue band is for $Q^2 = 0$ (the data is from GlueX in 2019), the red band is for $Q^2 = 1.2^2$ GeV$^2$, the green band is for $Q^2 = 2.2^2$ GeV$^2$.

# Electroproduction of heavy mesons near threshold

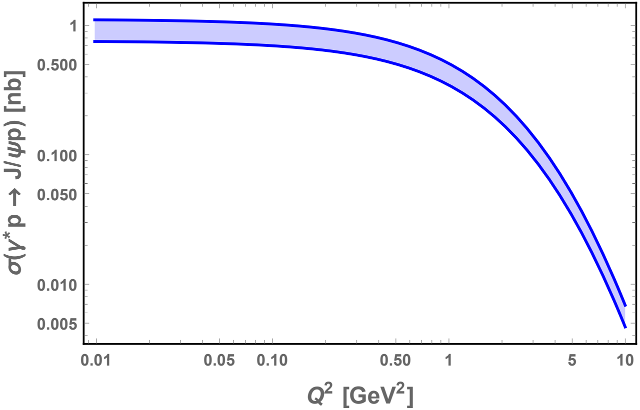


Figure: The variation of the total cross section with $Q^2$ (near threshold), s=$W^2 = 4.4^2$ GeV$^2$.

# Electroproduction of heavy mesons near threshold

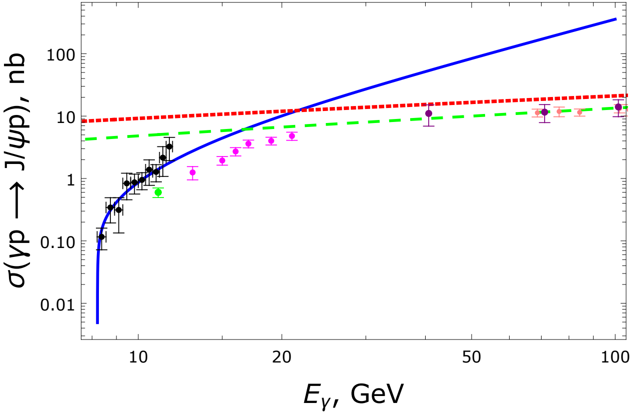


Figure: The total cross section for $J/\Psi$ photoproduction.

# Witten diagrams for $\gamma^{(*)} p \to \pi^0 p$

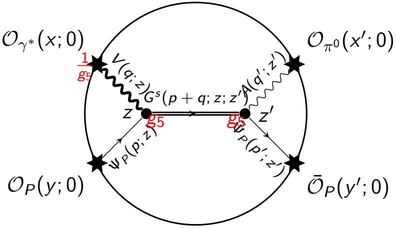


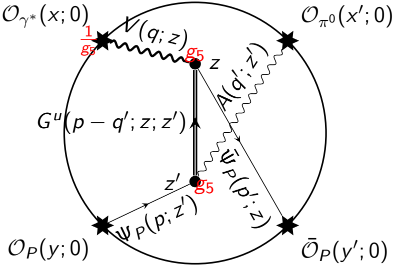


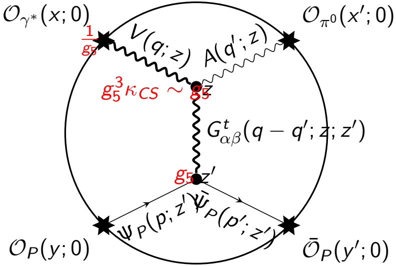

**Unified amplitude**

$$\mathcal{M}_{\gamma^{(*)}p\to\pi^0 p} = F_t(Q^2,s,t)\,M_t + F_s(Q^2,s)\,M_s + F_u(Q^2,u)\,M_u,$$

with soft-wall form factors

$$F_t(Q,s,t) = \frac{N_t\, g_5^3 \kappa_{\rm CS}\, g_5 c_\pi \kappa^2 \left[15 - \frac{Q^2}{4\kappa^2}\right]\Gamma(\tau)}{4\kappa^2\,\Gamma\!\left(\frac{Q^2}{4\kappa^2}+4\right)\Gamma\!\left(\frac{Q^2}{4\kappa^2}+1\right)^{-1}}$$
$$\times \frac{-t/(4\kappa_t^2)+2\tau}{\Gamma\!\left(-t/(4\kappa_t^2)+\tau+1\right)\Gamma\!\left(-t/(4\kappa_t^2)+1\right)^{-1}}\,\frac{1}{E_\pi^3},$$

$$F_s(Q,s) = \frac{N_s\, g_5 c_\pi \kappa^2 \left[\tau(2\tau-1)+(\tau-1)\frac{Q^2}{4\kappa^2}\right]\Gamma(\tau)}{4\,(M_0^2-s)\,\Gamma\!\left(\frac{Q^2}{4\kappa^2}+\tau+1\right)\Gamma\!\left(\frac{Q^2}{4\kappa^2}+1\right)^{-1}}, \qquad F_u = F_s\,(s\to u).$$

- ***t***–channel fixed by the Chern–Simons term dominates forward angles.
- ***s*, *u*** Born towers (infinite baryon spectrum) become relevant for $|t| \gtrsim 1\ \mathrm{GeV}^2$.
- Veneziano duality prevents double counting when all three channels are combined.

# Model vs. data (JLab CLAS / Hall A)

- Forward-angle structure functions $U = T + \varepsilon L$, $LT$, $TT$ reproduced in all 18 $(Q^2, W)$ bins with a *single* $F_t$.

$$\frac{d\sigma_T}{dt} = A_T + B_T \cos\theta + C_T \cos^2\theta + D_T \cos^3\theta$$

- Regge-resummed $F_t$ gives the correct $\sigma_T(Q^2, W)$ without extra parameters.
- Large-$|t|$ photoproduction requires $s + u$ Born terms explains "shoulder/dip" near $|t| \simeq 0.5$ GeV$^2$.
- Fit coefficients $(N_t, N_s, \kappa_t)$ are stable across kinematics.

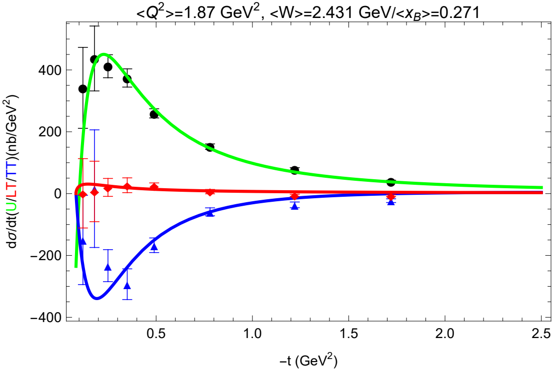


Figure: FIG. 2(a): $W \simeq 2.43$ GeV bin— $U$, $LT$, $TT$ vs. $-t$. Points: CLAS/Hall-A data; curves: holographic $t$-channel fit.

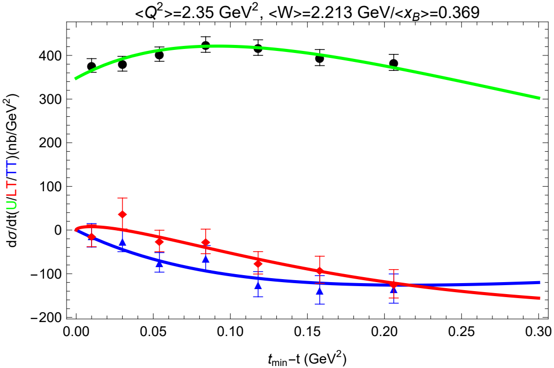


Figure: FIG. 2(b): $W \simeq 2.21$ GeV bin— same legend as (a).

# Total $\pi^0$ electroproduction cross sections

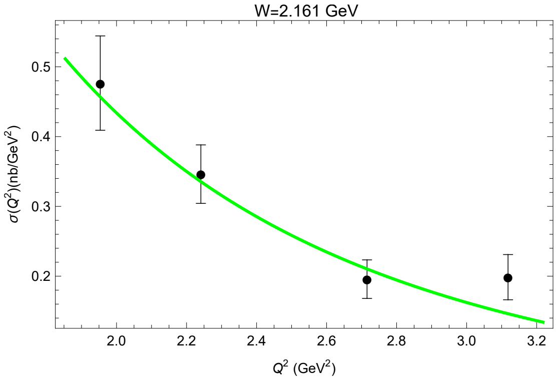


Figure: FIG. 3(a): $\sigma_T$ vs. $Q^2$ at $W \simeq 2.16$ GeV.

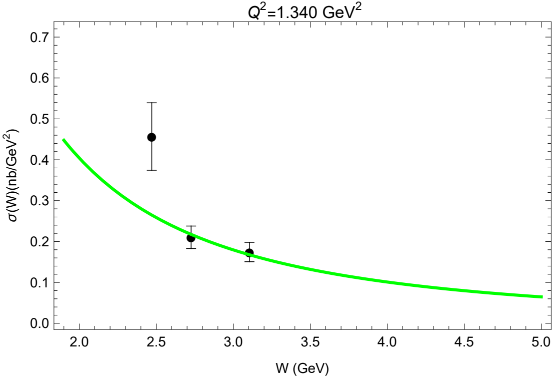


Figure: FIG. 3(b): $\sigma_T$ vs. $W$ at $Q^2 \simeq 1.34$ GeV$^2$.

# Photoproduction from forward to backward angles

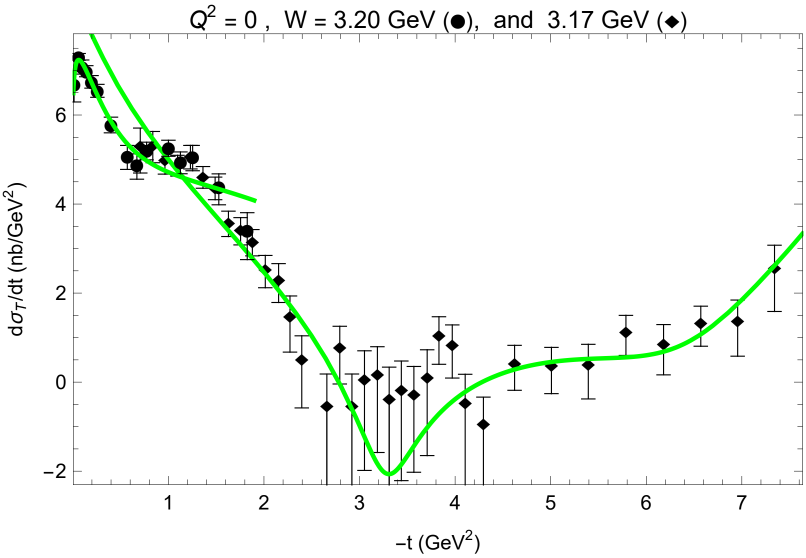

# Summary

- **Holographic dictionary.** Soft-wall AdS/CFT maps QCD currents and hadrons to bulk fields $V, A, \Psi$ (spin-1), $h$ (spin-2) and $f$ (spin-0); correlation functions and amplitudes are computed with Witten diagrams.
- **Nucleon structure.** Unified treatment of spin-1 *and* spin-2/0 form factors: EM FFs fixed by vector towers; gravitational FFs from $2^{++}$ / $0^{++}$ glueball exchange reproduce lattice and phenomenology.
- $\pi^0$ **electro/photoproduction.** Single amplitude $F_t + F_s + F_u$ — CS-driven $t$-channel + Veneziano-dual $s, u$ Born towers — fits CLAS/Hall-A structure functions and world photoproduction data with one parameter set.
- **Heavy-quarkonium near threshold.** $J/\psi$, $\Upsilon$ production isolates gluonic GFFs through $2^{++}$ and $0^{++}$ glueball exchange; holographic amplitude matches JLabJ/$\psi$-007 and GlueX cross sections.
- **Regge regime.** BPST kernel (strong-coupling analogue of BFKL) links small-$x$ four-point functions to GPD moments.
- **Complementarity.** Holographic QCD offers a comprehensive, self-contained framework that complements GPD factorization, providing unified insight into exclusive *and* inclusive processes at JLab and the future EIC.

# Thank You!